J. Fluid Mech. (1988), *vol.* 193, *pp.* 151–170
Printed in Great Britain

Monolayer flow on a thin film

By MICHAEL S. BORGAS AND JAMES B. GROTBERG

Biomedical Engineering Department, The Technological Institute, Northwestern University, Evanston, IL 60208, USA and Department of Anesthesia, Northwestern University Medical School, Chicago, IL, USA

(Received 19 January 1987 and in revised form 10 December 1987)

Two-dimensional flow of a surface-active monolayer on a thin viscous film is considered. Simplifications of negligible gravity and pressure forces are made. Interfacial properties are described by simple model equations of state. Solutions are obtained for when the monolayer is scraped along the interface by a barrier and a steady state exists where surface advection is balanced by surface diffusion. Surface velocity, film thickness and spreading rate dependence on surface diffusivity are examined.

1. Introduction

A fundamental property of the lung is the surface-tension characteristics of its liquid lining which exert global effects on pulmonary function (West 1979). A well-known feature of an air-cycled lung is its pressure-volume hysteresis loop. When the lung is liquid-cycled, this loop nearly closes and the lung's compliance increases, thus implicating the importance of the interfacial mechanics (Von Neergaard 1929). Surface-tension-area loops of cycled interfaces which contain surface-active agents similar to those in the lung (Bienkowski & Skolnick 1972) strongly reflect the corresponding pressure-volume loops, particularly their dynamic response (Grotberg, Mitzner & Davis 1980). Although this aspect of lung physiology has drawn a good deal of attention, little work has been done to study how these interfacial forces may be influenced by inhaled substances, especially liquid aerosols, or harnessed for medical purposes.

When a drug or toxin is dissolved in aerosol droplets, those solutes that are poorly soluble or absent in the gas phase can only reach the circulation by direct aerosol contact with the lung's liquid lining. In addition to the delivery of medical aerosols, many types of hazardous environments are found in the industrial setting, where oil mists and other airborne contaminants are encountered by humans (Schreck 1982). The dynamics of the droplet interaction with the lining is an important aspect of this transport problem that has not previously been investigated. An approach toward this phenomenon based on the fluid mechanics of the system should give useful information about the droplet-lining interaction which can form a basis for designing experiments necessary to evaluate the mechanics and transport phenomena related to surface-active material inhaled into the lung.

The study of one liquid spreading upon another has been pursued previously by Di Pietro, Huh & Cox (1978); Di Pietro & Cox (1979, 1980) and Foda & Cox (1980) who deal mainly with deep substrate-fluid layers, compared to the contaminant. Unlike these models, in the lung the droplet and lining can have comparable thicknesses. These studies provide a fairly comprehensive overview of the interfacial mechanics and all introduce the concept of a thin, monomolecular spreading layer

above part of the substrate. The intermolecular forces then give rise to interfacial tension variation and therefore to surface tractions. However, with a deep substrate, resistive forces due to viscous drag of the substrate fluid is smaller, compared to that due to a thin-layer substrate, and therefore spreading rates are faster. Consequently, slow processes like surface diffusion in the interface may be ignored when considering those flows. Many other concepts developed in the 'thick-layer studies' are, however, useful when the substrate layer is thin since the corresponding studies of that situation (Levich 1962; Yih 1969; Adler & Sowerby 1970; Ahmad & Hanson 1972; Hussain, Fatima & Ahmad 1975) are less well developed, both theoretically and experimentally. The first three thin-layer publications solve the same types of problems, with increasing geometrical complexity, and consider flows where the entire substrate is covered by a molecularly thin layer (i.e. with no droplet on the substrate) which greatly simplifies the description of the interfacial properties. The latter two papers mainly give experimental results.

With the exception of Adler & Sowerby's work, all of the studies, including the experimental work, deal with two-dimensional geometries. This work is also restricted to two dimensions. Additionally, many of the studies deal with steady-state motions, requiring special conditions so that such a state is established. Considering such flows is a useful first step in the development of the subject, though not a comprehensive one, and this approach is adopted for most of what follows. Some of the recent deep-layer studies (particularly Foda & Cox 1980) consider more general unsteady motions and experiments presented by Ahmad & Hanson (1972) deal with unsteady effects.

With the scales relevant for deep-layer spreading, surface diffusion is not an important process, however, for thin-layer spreading some account of this transport mechanism is warranted. Previous work reflects this fact and while none of the deep-layer studies consider surface diffusion, most thin-layer studies do. For thin-layer flows the limit of small diffusion is singular in the sense that neglecting such surface-transport processes leads to mathematical solutions which are not smooth, as we show below. Including surface diffusion 'smoothes out' the flow, but other effects such as capillarity forces may accomplish this also. Here, we consider only the influence of surface diffusion. It is interesting to note that neglecting surface diffusion does not lead to obviously singular solutions for any of the thick-layer flows, reflecting the relative unimportance of surface diffusivity in those cases.

In the following sections the dynamics of a single drop spreading on a thin film of a second fluid is considered. It is designed to be a general model that represents this category of problems rather than the lung system itself. Specific assumptions which deviate from the properties of the lung lining represent potential modifications that further modelling could employ. For the present purposes, this first primitive analogue will be sufficiently complicated and instructive. The most important physical result sought is the spreading rate of the deposited aerosol, the rate at which surface area is engulfed by the spreading drop, since the proportion of lung area affected will determine the extent of the response. The goal, therefore, is to categorize the spreading rate in terms of simple parameters which may be measured *in vitro*, or inferred *in vivo*, for a variety of compounds likely to be encountered.

2. The model problem

We model the film as a thin layer above a flat wall, since the airway wall radius of curvature is typically very large compared to the film thickness. We treat the

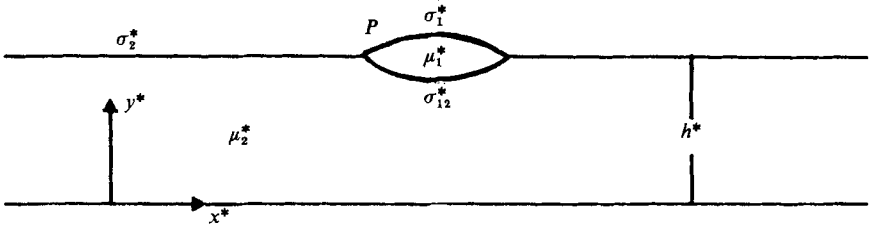

FIGURE 1. Schematic of a two-dimensional droplet on the surface of a thin fluid layer above a rigid wall.

lining fluid as Newtonian, using a subscript 2 to signify its properties, and assume that σ_2^* is constant for our model problem. Both of these asumptions deviate from the actual lung system, but allow us to address the underlying fluid dynamics pertinent to our simpler model. Suppose now that the surface is exposed to an insoluble aerosol droplet, which has characteristic surface tension σ_1^* at its air interface and σ_{12}^* at the interface between the aerosol droplet and the liquid lining. Figure 1 depicts the assumed two-dimensional geometry. Equilibrium of the droplet configuration depends upon the parameters σ_1^*, σ_2^* and σ_{12}^* according to the parameter S^* where

$$S^* = \sigma_2^* - \sigma_{12}^* - \sigma_1^*, \tag{2.1}$$

and S^* is termed the spreading coefficient, used and defined by many authors (Foda & Cox 1980; Adamson 1967; Gaines 1965; Harkins 1952). If $S^* > 0$, the droplet spreads and if $S^* < 0$, the droplet contracts. Clearly we are interested in problems where $S^* > 0$ as spreading drops have the potential to participate in transport due to convection and consequently exert a greater influence.

Given that spreading occurs it is apparent that a net outward force would act at the point P in figure 1. However, this would imply that an unacceptably large stress (force per unit area) acts in the neighbourhood of P. It has been suggested that a thin layer of fluid comprised of the aerosol molecules extends from P onto the lining. The layer is so thin that it is best considered as a surface concentration, Γ^*. This allows the surface tension to vary smoothly from the clean-surface value to the value of the combined tensions at P. Such thin layers are generally called monolayers although this is only literally correct for $\Gamma^* < \Gamma_c^*$, Γ_c^* being the critical surface concentration at which aerosol molecules are effectively close packed in a two-dimensional lattice. The coupled monolayer-drop system has no unacceptably large stresses and the forces generated by surface tractions may, in principle, be balanced by fluid mechanical forces and therefore spreading rates can be determined. As is evident later, monolayer dynamics are of particular importance since the drop's molecules are all in the monolayer state, given enough 'clean' surface on which to spread. It is interesting to note the analogy with a moving contact-line problem on a solid surface, as discussed by Dussan V & Davis (1974), Greenspan (1978) and Cox (1986), amongst others. There, an infinite stress is predicted at the contact line on the solid surface, however, it is not widely accepted that an analogue of the monolayer resolves the ensuing spreading paradox.

To study the nature of monolayer-droplet spreading, and to examine the effect of the principle forces in the system, we consider the system in a reference frame in which the motion appears to be steady. Equivalently, this can be considered as a problem with a moving wall beneath the liquid lining. The fluid stresses generated by

the moving wall balance the stresses at the interface. To achieve such a steady state requires artificial boundary conditions at the drop. Some collection of forces must be imposed to hold the droplet or terminal end of the monolayer stationary with respect to the new reference frame. In fact, in the original reference frame the drop moves, e.g. is being 'scraped' along the surface. Thus any estimate of the spreading rates, by assuming quasi-steady motion for instance, will be an overestimate because of the additional artificial forcing. Nevertheless, the problem serves as a soluble introduction into the dynamics of the system.

3. Monolayer dynamics

The fluid motions within the liquid lining are governed by the Navier–Stokes equations; if $(u^*(x^*, y^*, t^*), v^*(x^*, y^*, t^*))$ is the velocity vector and $p^*(x^*, y^*, t^*)$ is the pressure in the fluid, then

$$\rho_2[u^*_{t^*} + u^* u^*_{x^*} + v^* u^*_{y^*}] = -p^*_{x^*} + \mu_2^*(u^*_{x^*x^*} + u^*_{y^*y^*}), \tag{3.1}$$

$$\rho_2[v^*_{t^*} + u^* v^*_{x^*} + v^* v^*_{y^*}] = -p^*_{y^*} + \rho_2^* g^* + \mu_2^*(v^*_{x^*x^*} + v^*_{y^*y^*}), \tag{3.2}$$

and conservation of mass is satisfied when

$$u^*_{x^*} + v^*_{y^*} = 0. \tag{3.3}$$

Boundary conditions which complement (3.1)–(3.3) are that there is no flow of fluid through the rigid wall nor through the interfaces and, finally, that stresses balance at the interfaces between fluids. These relationships will be given explicitly below.

Given that spreading occurs an obvious simplifying feature is the lengthscale along the lining versus its resting thickness, h^*. Lubrication theory approximations are therefore suitable so that the equations above may be approximated by

$$\mu_2^* u^*_{y^*y^*} \approx p^*_{x^*}. \tag{3.4}$$

The solution for v^* follows from the equation of continuity (3.3) and from solving for u^* in (3.4). The pressure p^* is at most a linear function of y^*, which follows from the lubrication approximations applied to (3.2), and where the coefficients are prescribed by boundary conditions. Note that the pressure gradient $p^*_{x^*}$ is independent of y^*, therefore the horizontal velocity is approximately a quadratic function of y^*, where the coefficients of each power of y^*, functions of x^* and t^*, remain to be determined.

The driving forces, gravity, capillarity and tangential stress gradients at the interface, are balanced by viscous forces in the liquid lining and the additional dissipative effects associated with the interface, i.e. surface viscosities. Fluid inertia in the lining and in the surface is negligible in the balance of forces. These effects may be estimated from (3.1) and (3.2) where the terms on the left represent inertial acceleration of fluid particles; the relative importance of these terms is discussed below.

Let $y^* = H^*(x^*, t^*)$ define the height of the liquid lining above the rigid wall $y^* = 0$, where the superscript * generally signifies dimensional quantities. The pressure acting on the fluid, just below the interface, is given approximately by

$$p^*|_{H^*} = -\sigma^* H^*_{x^*x^*}, \tag{3.5}$$

while the pressure acting just above the surface is a constant, say 0. From the lubrication approximations the pressure throughout the liquid lining may be written as

$$p^*(x^*, y^*, t^*) = \rho_2^* g^*(H^* - y^*) - \sigma^* H^*_{x^*x^*}, \tag{3.6}$$

and hence the pressure gradient is given by

$$p^*_{x^*}(x^*, t^*) = \rho_2^* g^* H^*_{x^*} - (\sigma^* H^*_{x^*x^*})_{x^*}. \tag{3.7}$$

Also, there is a balance of tangential fluid stresses exerted on the interface $y^* = H^*(x^*, t^*)$ with surface-tension gradients and additional stresses from surface viscosity, i.e.

$$\mu_2^* u^*_{y^*}|_{H^*} = \sigma^*_{x^*} + \frac{\mathrm{d}}{\mathrm{d}x^*}\left(\kappa^* \frac{\mathrm{d}}{\mathrm{d}x^*} u^*|_{H^*}\right), \tag{3.8}$$

where we have supposed that the interface monolayer behaves rheologically as a Newtonian interface (Scriven 1960). Note that for two-dimensional flows there is no two-dimensional shear in the plane of the interface, thus the stress that results is due to a dilational viscosity, $\kappa^* (> 0)$, multiplied by the rate of expansion of the interface.

Let $u_s^*(x^*, t^*)$ be the velocity of fluid at the interface. Then by virtue of the quadratic nature of $u^*(x^*, y^*, t^*)$ (with y^* variations), and the lubrication balance of stress in the substrate (equation (3.4)), u_s^* is governed by (3.8), giving

$$(\kappa^*(u_s^*)_{x^*})_{x^*} + \sigma^*_{x^*} = \mu_2^* \frac{u_s^*}{H^*}. \tag{3.9}$$

Having determined the surface velocity the complete velocity field may be written as

$$u^*(x^*, y^*, t^*) = \frac{1}{2\mu_2^*} p^*_{x^*} y^{*2} + \left(\frac{u_s^*}{H^*} - \frac{1}{2\mu_2^*} p^*_{x^*} H^*\right) y^*, \tag{3.10}$$

where no slip of fluid along the rigid plate is an imposed boundary condition. The remaining boundary conditions, those of purely kinematic nature, are best imposed by the following formulation: let q^* be the flux of monolayer material along the interface; and let Q^* be the flux of material (substrate fluid) between the rigid plate and the interface. Then we have

$$q^* = u_s^*(x^*, t^*)\, \Gamma^* - D^* \Gamma^*_{x^*}, \tag{3.11}$$

where the flux is due to advection (the first term) and diffusion (the second term), and

$$Q^* = \rho_2^* \int_0^{H^*} u^*(x^*, y^*, t^*)\, \mathrm{d}y^* \tag{3.12}$$

is a purely advective flux. Conservation of mass then requires that

$$\Gamma^*_{t^*} + q^*_{x^*} = 0, \tag{3.13}$$

and

$$\rho_2^* H^*_{t^*} + Q^*_{x^*} = 0; \tag{3.14}$$

where the first equation is for material in the interface, the second for material in the substrate layer.

Equations (3.13) and (3.14) are solved subject to some initial conditions and also some end conditions, which are described later. With these, the state of the spread at any subsequent instant is determined. However, the practical application of this system is complicated, particularly when the velocity u^* at each time instant requires explicit calculation from (3.9), due to surface viscosity. Thus, for an initial investigation, we ignore surface viscosity, $\kappa^* = 0$, and later the order of magnitude of the corrections due to a small finite κ^* is estimated. Secondly, we investigate conditions for steady-state solutions of the system.

4. A steady state flow

Suppose the flow is steady in a reference frame moving with constant velocity U_w^*, and furthermore that the coordinate axes are moving, fixed with the monolayer. Then we obtain the fluid velocity in the liquid lining from (3.9) as

$$u^*(x^*, y^*) = \frac{1}{2\mu_2^*} p_{x^*}^* (y^{*2} - 2y^* H^*) + \frac{1}{\mu_2} \sigma_{x^*}^* y^* + U_w^*, \tag{4.1}$$

where $p_{x^*}^*$ is given by (3.3). The mass flux of material in the liquid lining, from (3.12), may be written as

$$\frac{Q^*}{\rho_2^*} = -\frac{1}{3\mu_2^*} p_{x^*}^* H^{*3} + \frac{1}{2\mu_2^*} \sigma_{x^*}^* H^{*2} + U_w^* H^*. \tag{4.2}$$

Moreover, to conserve mass,

$$Q^* = \rho_2^* h^* U_w^*, \tag{4.3}$$

where the right-hand side is the mass flux of liquid lining adhering to the moving wall far upstream (as $x^* \to -\infty$) where the interface is both flat and relatively uncontaminated.

Also of importance, with respect to transport of the interfacial contaminant, is the surface velocity u_s^*, where

$$u_s^*(x^*) = -\frac{1}{2\mu_2^*} p_{x^*}^* H^{*2} + \frac{1}{\mu_2^*} \sigma_{x^*}^* H^* + U_w^*. \tag{4.4}$$

The mass flux of contaminant along the interface is then given by (3.11) coupled with (4.4). Far upstream $q^* = 0$, because the surface there is uncontaminated. Then by virtue of insolubility of the contaminant and to conserve mass,

$$q^*(x^*) = 0, \tag{4.5}$$

everywhere on the interface. Finally, given equations of state for $\sigma^*(\Gamma^*)$ and $D^*(\Gamma^*)$ (see §6 below), (4.1) and (4.4) together with the flux constraints allow, in principle, for the calculation of H^* and Γ^* as functions of x^*. Then some measure of monolayer length, to be made precise later, is available as a function of U_w^* and this is the main result of practical significance.

5. Dimensional scalings

It is convenient to consider flow quantities as dimensionless multiples of chosen reference scales. Clearly velocities may be measured relative to U_w^*, heights relative to h^* and, less obviously, lengths relative to $L^* = (S^*/U_w^* \mu_2^*) h^*$. The latter lengthscale represents an emphasis on balancing surface-tension gradients with

viscous shear stresses. Implicit in the work so far is the lubrication asumption, for this to be valid we must have $h^*/L^* = \lambda \ll 1$. In particular, this means that only wall velocities much smaller than S^*/μ_2^* (≈ 1 cm s^{-1} as estimated below) can be considered. Lastly, the surface concentration is measured relative to Γ_c^* although this is completely arbitrary as this parameter does not appear in any critical way. The principle equations, in non-dimensional form (with superscripts * suppressed), are:

$$-\tfrac{1}{3}p_x H^3 + \tfrac{1}{2}\sigma_x H^2 + H = 1, \tag{5.1}$$

and

$$(-\tfrac{1}{2}p_x H^2 + \sigma_x H + 1)\Gamma - \delta D\Gamma_x = 0, \tag{5.2}$$

where the pressure gradient is given by

$$p_x = (\alpha H_x - \lambda^2([\hat{\gamma} + \sigma]H_{xx})_x. \tag{5.3}$$

The dimensionless surface tension is $\sigma^*/S^* = \hat{\gamma} + \sigma$ and the scaled surface diffusivity is $D = D^*/D_0$. The end conditions for this system of equations, at the extremities of the monolayer, are that $\Gamma = 0$ at the leading 'edge' of the monolayer, while $\Gamma \to \infty$ near the bulk-droplet-monolayer boundary.

The key non-dimensional parameters which now appear as given as:

$$\alpha = \frac{\rho_2^* g^* h^{*2}}{S^*}, \quad \hat{\gamma} = \frac{\sigma_1^* + \sigma_{12}^*}{S^*}, \quad \delta = \frac{D_0^* \mu_2^*}{S^* h^*},$$

where D_0^* is the (constant) dilute diffusion coefficient. Notice that the capillary term in (5.3) is necessarily small provided that the lengthscale for surface-tension variations is sufficiently large; equivalently, that S^* is not too small. Therefore, capillary forces are generally only important at the ends of the monolayer in some axial boundary-layer region at the bulk droplet and at the tip of the monolayer. Note that this also means that the dimensions of the drop, supposing that it is held principally by capillary forces, will have much smaller horizontal scales than the typical monolayer scales and therefore may be approximated as the neighbourhood of a point. Additionally, this means that the dynamics of the drop are of lesser importance in as much as total contaminated area is concerned.

Typical values of the parameters may be estimated by taking, for instance, the values $\rho_2^* = 1$ g cm^{-3}, $g^* = 980$ cm s^{-2}, $\sigma_2^* = 40$ dyn cm^{-1} (average), $S^* = 10$ dyn cm^{-1}, $\mu_2^* = 10$ Poise (large) and with $h^* = 10^{-1}$ μm (small). In all but the most extraordinary circumstances, say with $S^* \ll \sigma_2^*$ (a case of little practical significance), the parameters α and λ are both very small ($< 10^{-4}$), where $O(1)$ values are anticipated to indicate physical significance. The only parameter above which may be important is δ. However, surface diffusivities are difficult to measure and generally small. Nevertheless, taking a value of $D_0^* = 10^{-5}$ cm^2 s^{-1} leads to a value of $\delta = 1$, indicating probable significance. Moreover, experimental measurement of surface diffusion find that such values of D_0^* are not unreasonable (Sakata & Berg 1969). More extreme parameter values, e.g. larger viscosity and thinner lining thickness, tends to enhance δ, therefore the mechanism of surface diffusion warrants investigation. In contrast, to enhance the other parameters to $O(1)$ values requires more 'exotic' mechanical properties of the liquid lining.

The surface–viscosity effect mentioned above, may be categorized by the parameter κ, which gives the order of magnitude of the surface–viscosity stresses relative to surface-tension gradients. Scaling equation (3.9) yields the dimensionless parameter

$$\kappa = \frac{\kappa^*}{h^* \mu_2^*} \lambda^2.$$

Then with the values given above and for surface viscosities of the order of 10^{-3}–10^{-1} surface Poise (typical for most liquids) non-dimensional corrections to the flow field will be of $O(100\lambda^2)$. According to the lubrication approximation, κ is small enough if λ is small enough and we shall suppose that it is. Initially, however, immediately after droplet deposition, when $\lambda \approx O(1)$, it appears that surface-viscosity effects are significant.

Finally we consider the inertia terms which are neglected at leading order in the lubrication approximation. From (3.1) and (3.2) these are proportional to

$$\frac{\rho_2^* U_w^* h^*}{\mu_2^*}\lambda = Re\,\lambda,$$

where Re is the Reynolds number based on layer thickness (and which itself is small), therefore the inertia terms are always small.

6. Equations of state

To make further progress it is necessary to assume that the local surface tension and local surface diffusivity are functions of the local surface concentration (i.e. the local state of the interface). Accordingly we write

$$\sigma = \sigma(\Gamma), \quad D = D(\Gamma),$$

as the equations of state. Quantitative experimental tabulation, or theoretical estimates, of these relationships is difficult and, particularly for the latter, rare. However, in the dilute-surface-concentration limit, as $\Gamma \to 0$, we have $\sigma \to 1$ and $D \to 1$ because of the choice of scales. Also we extend the domain of validity of the 'monolayer' state beyond the point of 'close packing', i.e. $\Gamma = 1$. In particular, we assume that $\sigma \to 0$ as $\Gamma \to \infty$, i.e. in the limit of 'infinite' surface concentration the tension appropriate for a bulk droplet is attained by the extended monolayer. Almost all surface chemistry ignores the extended monolayer domain. Equations of state for $\Gamma < 1$ are reasonably well documented (e.g. Adamson 1967; Gaines 1966). Foda & Cox (1980) determine an extended surface-tension equation of state for an oil layer on water; thus, in principle, such measurements are possible and therefore equations of state are assumed to exist for all Γ. Foda's results are shown in figure 2, and are for an oil layer (Dow Silicone 100 cP oil) on water. Furthermore, regarding $\sigma(\Gamma)$, the theoretical behaviour for large Γ, i.e. the form as $\Gamma \to \infty$, follows from Sheludko (1966) and must behave like $\sigma(\Gamma) \simeq \Gamma^{-3}$. Thus we assume that

$$\sigma(\Gamma) = (1+\theta\Gamma)^{-3}, \tag{6.1}$$

where θ is an empirical constant, models the surface tension adequately. Shown on figure 2 is a sample equation of state with $\theta = 0.15$ in (6.1). In fact, the parameter θ is determined by simple material properties of the monolayer constituent. From Adamson (1967) monolayers in the dilute concentration limit, so called gaseous expanded monolayers, follow the (dimensional) 'law'

$$\sigma^* = \sigma_2^* - \frac{R^*T^*}{M^*}\Gamma_1^*,$$

where R^* is the gas constant, T^* is the temperature (assumed constant) and M^* is the molecular weight of the monolayer material, from which β is prescribed.

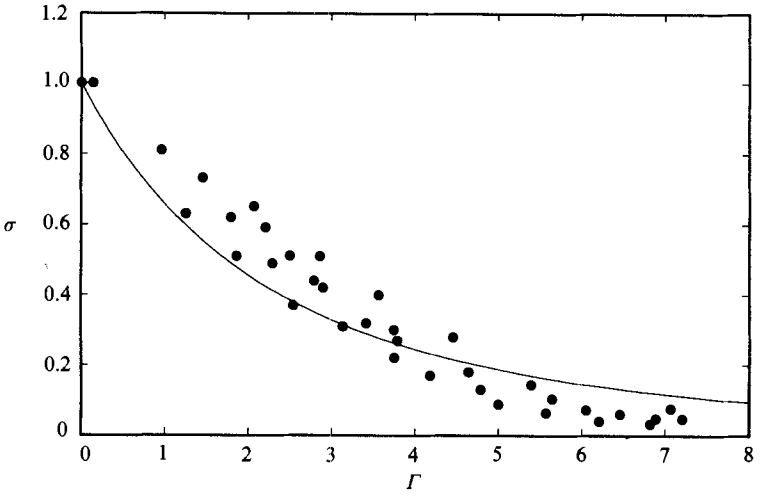

FIGURE 2. Foda & Cox's equation of state (experimental data points (●)) and a curve from the model equation of state (6.1) with $\theta = 0.15$.

Results for surface-diffusion properties are less well documented but the results of Sakata & Berg (1969) are useful. Therefore we examine several alternative choices for $D(\Gamma)$ and attempt to find reasonably general results. Let

$$D(\Gamma) = (1+\tau\Gamma)^{-n} \tag{6.2}$$

be an equation of state for diffusion. n and τ are empirical parameters, which both satisfy $n, \tau > 0$. Equation (6.2) embodies most of the essential physics: firstly, the 'correct' dilute limit; and secondly, disenhancement of diffusion as surface concentration increases because the mobility of molecules in the interface becomes increasingly impeded. This effect was investigated by Sakata & Berg (1969) who measured diffusivity for a 'gaseous' monolayer and for an 'intermediate' monolayer film, a monolayer state for larger surface concentrations and not described by the linear 'law' given above, and found the diffusivity correspondingly reduced in the latter case.

An alternative law, emphasizing the disenhancement effect explicitly, is given below, where the diffusive mechanism 'switches off' at the close-packing limit of surface concentration:

$$\begin{aligned} D(\Gamma) &= (1-\Gamma)^n \quad (\Gamma \leqslant 1), \\ &= 0 \qquad\quad (\Gamma > 1). \end{aligned} \tag{6.3}$$

The equations of state expressed by equations (6.1)–(6.3) may be expected to govern fairly wide classes of monolayers.

7. Surface-tension-gradients/surface-diffusion solution

When the pressure gradient and surface diffusion terms are ignored in (5.1) and (5.2), the solution and the flow that it represents is trivial. We then have, for the region covered by a monolayer, between $\sigma = 0$ and $\sigma = 1$,

$$\sigma_x(x) = -\tfrac{1}{2}, \quad u_s(x) = 0, \quad H(x) = 2,$$

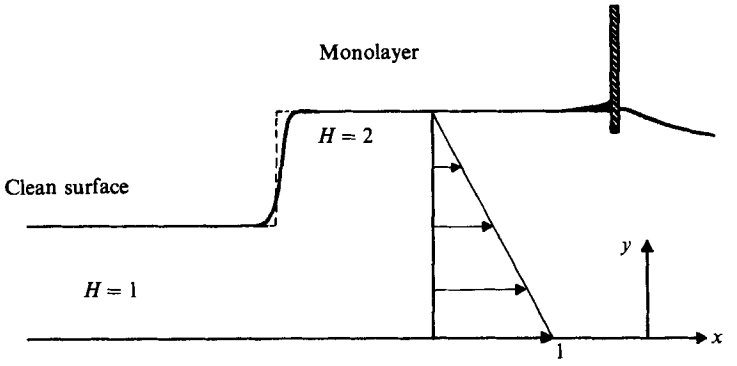

FIGURE 3. Schematic of a steady flow with a moving wall and with a monolayer held stationary. Surface diffusion is negligible (almost everywhere).

all constants for all such x. By virtue of the constant gradient of σ, the monolayer exists over a finite length from $x = -L$ to $x = 0$. The monolayer in this case acts as a rigid plate of length $L = 2$. Ahead of the monolayer, extending to infinity, the flow is simply represented by

$$\sigma(x) = 1, \quad u_s(x) = 1, \quad H(x) = 1 \quad (\text{for } x < -L \text{ say}).$$

Figure 3 illustrates the flow and the discontinuous transition at the leading edge of the monolayer. Such behaviour is assumed to be 'smoothed out' by including the neglected terms when shorter lengthscales are appropriate. This is explicitly demonstrated below, when surface diffusion is included as a significant effect. In fact, when δ is $O(1)$ there is no discontinuous transition at all, and when δ is small the lengthscale on which the discontinuity is smoothed out is short, of length $O(\delta)$.

Suppose that we now account for surface diffusion. The equations governing the flow are

$$\tfrac{1}{2}\sigma_x H^2 + H = 1, \tag{7.1}$$

and

$$(\sigma_x H + 1)\Gamma = \delta D \Gamma_x. \tag{7.2}$$

Note that the pressure gradient within the fluid is still negligible (i.e. the parameters α and λ^2 are both small), therefore the pressure throughout the thin layer is, to leading order, that of the ambient 'atmospheric' pressure, so $p = 0$. End conditions for (7.1) and (7.2) are that

$$\sigma \to 1, \quad H \to 1, \quad \Gamma \to 0 \quad \text{as } x \to -\infty,$$

and

$$\sigma \to 0, \quad \Gamma \to \infty \quad \text{as } x \to 0,$$

where a possible arbitrary origin shift permits the latter statement. The equations of state, discussed in §6, complement the system and, together with the end (boundary) conditions, permit solutions to be obtained.

In contrast with the 'diffusionless' case the monolayer now extends an infinite distance upstream, the concentration diminishing exponentially with distance. A finite measure of length, L_e, is defined later so that quantitative comparisons with the diffusionless solution can be made. Note also that the surface velocity $u_s(x)$ is no longer zero along the monolayer. In fact advective transport is balanced by the diffusional transport, maintaining zero total transport.

Solution of (7.1) and (7.2) is facilitated by regarding all quantities as functions of σ and the x dependence then follows by knowing $\sigma(x)$, which is calculated below. Thus we arrive at

$$H(\sigma) = 1 - \tilde{\tilde{\delta}}(\sigma) + (1 + \tilde{\tilde{\delta}}^2(\sigma))^{\frac{1}{2}}, \tag{7.3}$$

obtained by eliminating σ_x from (7.1) and (7.2) then solving the resulting quadratic equation for H. This then leads to the relationship

$$\sigma_x(x) = -(1 + (1 + \tilde{\tilde{\delta}}^2(\sigma))^{\frac{1}{2}})^{-1}, \tag{7.4}$$

and where, in all of the above,

$$\tilde{\tilde{\delta}}(\sigma) = -\frac{\delta D(\sigma)}{\Gamma(\sigma)} \frac{\mathrm{d}\Gamma}{\mathrm{d}\sigma},$$

is related solely to the equations of state, with σ interpreted as the state variable, and the surface-diffusion parameter, δ. Some general properties of $\tilde{\tilde{\delta}}$ are:

$$\tilde{\tilde{\delta}} \simeq (1-\sigma)^{-1} \quad \text{as } \sigma \to 1, \quad \tilde{\tilde{\delta}} \simeq \sigma^{\frac{1}{3}n-1} \quad \text{as } \sigma \to 0,$$

(for equations of state like (6.2) where the parameter n is defined). If, for example, $n \leqslant 3$ the steady state solution could not exist, implying a non-zero velocity at the drop-monolayer boundary, which is assumed to be stationary in the present reference frame. In fact the surface velocity is given by

$$u_s(\sigma) = \tilde{\tilde{\delta}}(\sigma)\,(1 + (1 + \tilde{\tilde{\delta}}^2(\sigma))^{\frac{1}{2}})^{-1}, \tag{7.5}$$

which vanishes if, and only if, $\tilde{\tilde{\delta}} = 0$. Thus, for a steady solution to exist we are restricted to smaller classes of possible equations of state. Given such equations of state, the height of the substrate layer at the monolayer/droplet boundary is predicted to be $H = 2$, independent of equations of state, so this is simply a statement of conservation of mass.

A useful property of the monolayer solution is a finite measure of monolayer length, say L_ϵ. ϵ is a small number (for practical purposes), and L_ϵ is chosen to be the length of monolayer state over which the (scaled) surface tension changes from 0 to $1-\epsilon$. Thus $L_\epsilon \to \infty$ as $\epsilon \to 0$. For our purposes $\epsilon = 0.05$ is useful. To determine the spatial structure of the solution we need σ as a function of x. This is given, implicitly, by integrating (7.4), i.e.

$$x(\sigma) = -\sigma - \int_0^\sigma (1 + \tilde{\tilde{\delta}}^2(\sigma'))^{\frac{1}{2}} \mathrm{d}\sigma', \tag{7.6}$$

where, as noted earlier, it is possible to define $x(0) = 0$ as the origin. An explicit expression for L_ϵ, therefore, is

$$L_\epsilon = 1 - \epsilon + \int_0^{1-\epsilon} (1 + \tilde{\tilde{\delta}}^2)^{\frac{1}{2}} \mathrm{d}\sigma. \tag{7.7}$$

While many possible forms of $\tilde{\tilde{\delta}}(\sigma)$ allow for explicit integration of (7.6) and (7.7), it is more convenient to calculate these integrals numerically, which allows $\tilde{\tilde{\delta}}(\sigma)$ to be taken in a more general form. For this task we use Simpson's rule (see Abramowitz & Stegun 1972, p. 886) to integrate, and choose two discretization step sizes, h and $2h$ (where typically $h = 0.001$) then extrapolate to obtain accurate results.

Figures 4 and 5 show results for $\sigma(x)$, for several values of δ, and the respective 'equations of state' (described below)

$$\tilde{\tilde{\delta}} = (\tfrac{1}{3}\delta)\,\sigma^{\frac{1}{3}}(1-\sigma^{\frac{1}{3}})^{-1} \quad (n = 4),$$

and

$$\tilde{\tilde{\delta}} = (\tfrac{1}{3}\delta)\,\sigma(1-\sigma^{\frac{1}{3}})^{-1} \quad (n = 6).$$

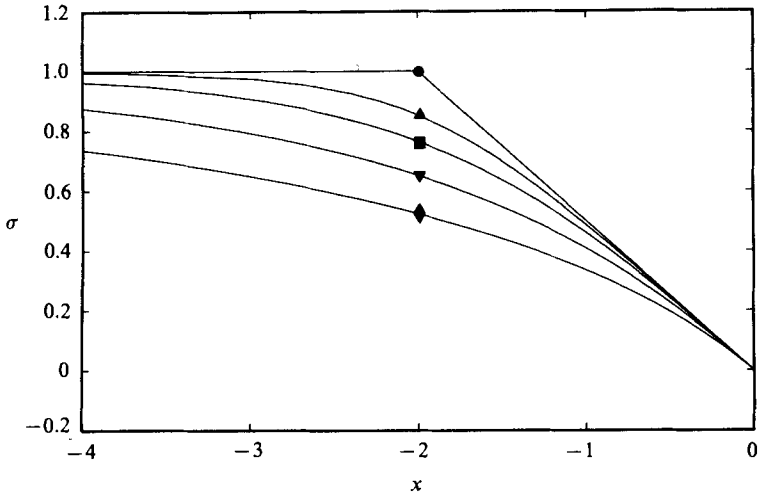

FIGURE 4. Results for surface-tension variations, $\sigma(x)$, for the monolayer covered region; equations of state (6.1) ($\theta = 1$) and (6.2) ($n = 4, \tau = 1$) and for diffusion parameter δ: $\delta = 0.0$(●), 0.5(▲), 1.0(■), 2.0(▼) and 4.0(◆) (increasing diffusivity).

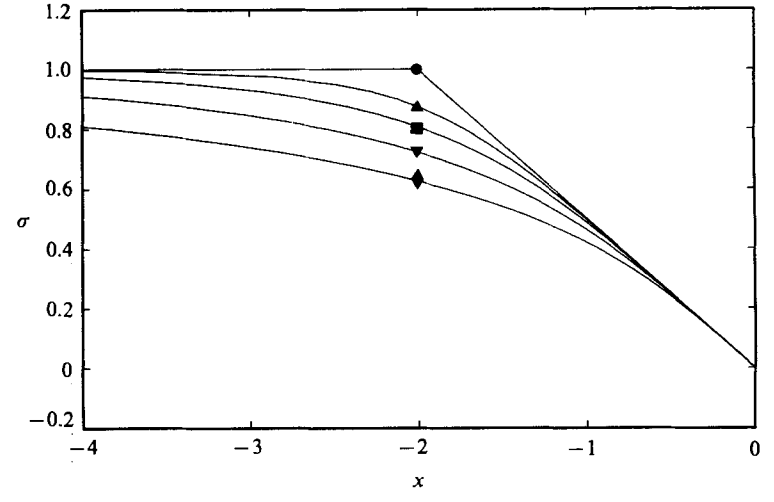

FIGURE 5. Results for surface-tension variations, $\sigma(x)$, for the monolayer covered region; equations of state (6.1) ($\theta = 1$) and (6.2) ($n = 6, \tau = 1$) and for diffusion parameter δ: $\delta = 0.0$(●), 0.5(▲), 1.0(■), 2.0(▼) and 4.0(◆) (increasing diffusivity).

Note two things: firstly, any value of the diffusion parameter, δ, smooths out the discontinuity illustrated in figure 4; secondly, the upstream influence of the monolayer becomes increasingly significant as δ increases. Both these limits (i.e. small and large δ) are considered below in full detail. Corresponding results for the layer thickness and surface velocity, as functions of x, are given in figures 6–9, again showing the smooth transitions with finite surface diffusion. The equations of state used for the numerical work are obtained from §6 assuming the following: the parameters θ and τ are both unity and that the exponent n is, respectively, 4 and 6.

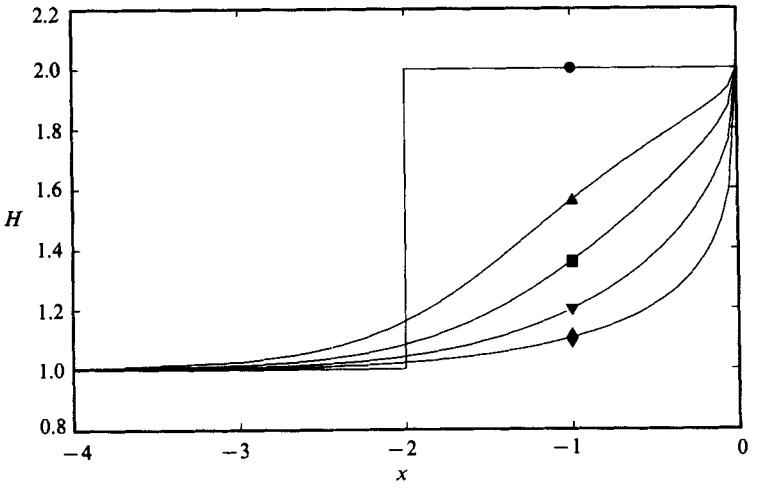

FIGURE 6. Results for substate height, $H(x)$, for the cases described in figure 4.

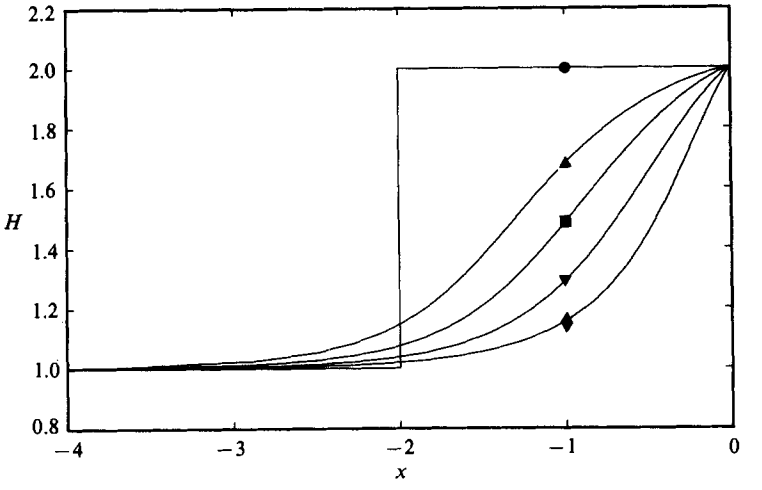

FIGURE 7. Results for substate height, $H(x)$, for the cases described in figure 5.

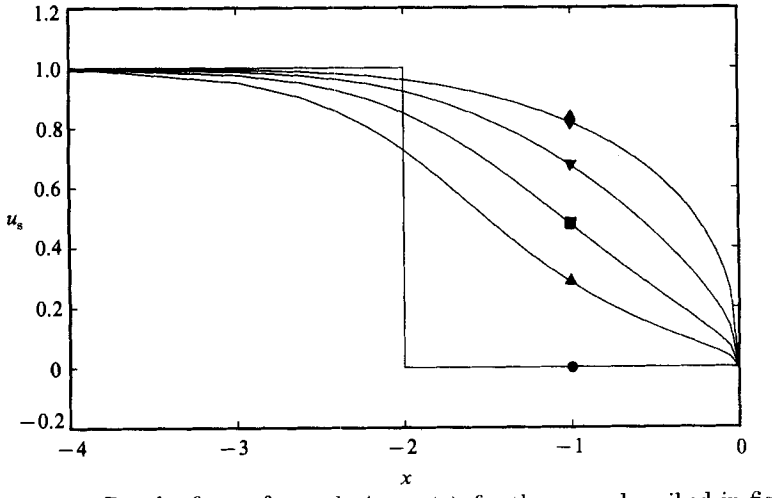

FIGURE 8. Results for surface velocity, $u_s(x)$, for the cases described in figure 4.

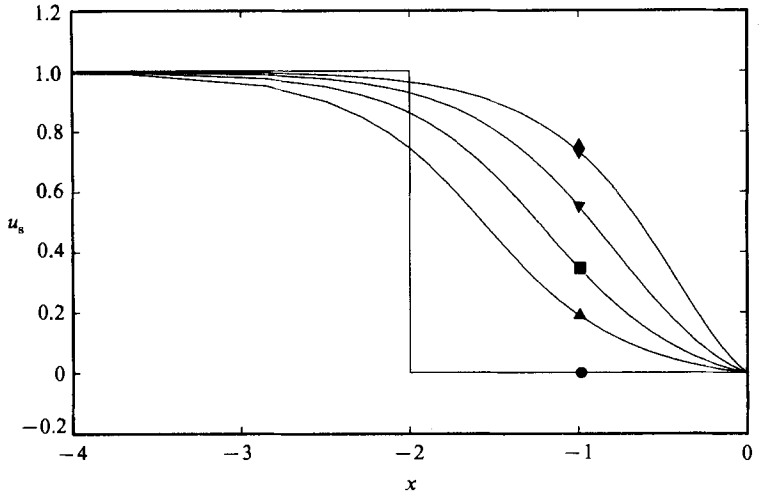

FIGURE 9. Results for surface velocity, $u_s(x)$, for the cases described in figure 5.

8. Asymptotic solutions

Explicit general results are available in both limits as either $\delta \to 0$ or ∞. Consider the first limit; δ small implies that, almost everywhere,

$$\sigma_x \approx -\tfrac{1}{2}, \quad H \approx 2,$$

except when the surface concentration is very small, which leads to

$$H \approx 1 \quad (\Gamma \approx 0).$$

Here we are restricted to $\alpha, \lambda^2(\hat{\gamma}+\sigma) \ll \delta \ll 1$. Thus as diffusion becomes less and less important for decreasing δ, the discontinuous solution described in the previous section is an increasingly good approximation. However, the solution is never really discontinuous, because near $\sigma = 1$ a new scale for variations becomes important. In general

$$\tilde{\delta} \simeq \delta(1-\sigma)^{-1}$$

when σ is near to 1, thus we put

$$\sigma = 1-\delta\tilde{\sigma}, \quad x = -2+\delta\xi,$$

then the local problem (about $x = -2$, where $\tilde{\sigma}$ and ξ are both $O(1)$), which describes the transition from $H = 1$ far upstream and $H \approx 2$ at the monolayer, is governed by the equations

$$H(\tilde{\sigma}) = 1-\frac{1}{\tilde{\sigma}}+\left(1+\frac{1}{\tilde{\sigma}^2}\right)^{\frac{1}{2}}, \tag{8.1}$$

and

$$\tilde{\sigma}_\xi(\xi) = \left(1+\left(1+\frac{1}{\tilde{\sigma}^2}\right)^{\frac{1}{2}}\right)^{-1}, \tag{8.2}$$

(from the corresponding equations (7.1) and (7.2)). The local spatial structure of the transition region is given by integrating (8.2); then

$$\xi(\tilde{\sigma}) = \tilde{\sigma}+(1+\tilde{\sigma}^2)^{\frac{1}{2}}+\log\left[\frac{\tilde{\sigma}+(1+\tilde{\sigma}^2)^{\frac{1}{2}}-1}{\tilde{\sigma}+(1+\tilde{\sigma}^2)^{\frac{1}{2}}+1}\right], \tag{8.3}$$

which gives

$$\xi \simeq \log(\tilde{\sigma}) \quad \text{as } \tilde{\sigma} \to 0,$$

i.e. the far upstream behaviour, with exponential decay of $\tilde{\sigma}$ (and Γ) with distance upstream, and

$$\xi \simeq 2\tilde{\sigma} \quad \text{as } \tilde{\sigma} \to \infty,$$

i.e. matching onto the tip of the monolayer where the tension varies linearly with distance (with slope approximately $-\frac{1}{2}$). Thus (8.3) clearly embodies the solution in the transition region. Therefore we have the leading-order structure for the steady solution, higher-order corrections depend strongly on the precise nature of the equations of state, and are anyway not important practically given the approximate nature of the problem.

From (8.3) it also follows that

$$L_\epsilon = 2 - \xi_\epsilon \delta \quad \text{where } \xi_\epsilon \simeq \log \epsilon - \log 2 + 1 + \ldots,$$

so that for ϵ small enough ξ_ϵ is negative and perhaps reasonably large. Therefore the effective monolayer length is increased to a relatively large degree by even a small surface diffusion effect.

Of less physical interest is the limit of large δ. Now, conversely, a new long lengthscale is appropriate for variations of monolayer quantities; consequently we put $x = \delta\xi$. Now $H \approx 1$ almost everywhere, but the surface tension varies with distance according to

$$\sigma_\xi(\xi) = -\delta \tilde{\delta}^{-1}(\sigma); \tag{8.4}$$

note that the right-hand side of (8.4) is independent of the parameter δ. Once again the solution may be obtained explicitly by quadrature, except in a small inner region about the monolayer/drop boundary where diffusive transport becomes smaller and the substrate-layer thickness varies appreciably. Thus near $\sigma = 0$ the solution is governed differently, on an inner lengthscale which is dependent on the equations of state, i.e. we put

$$\sigma = \delta^{-\beta}\hat{\sigma}, \quad x = \delta^{-\beta}\hat{\xi},$$

where $\beta = \frac{1}{3}n - 1$ and $\hat{\xi}, \hat{\sigma}\ O(1)$ describes the inner region. The equations governing the inner solution, again from (7.1) and (7.2) are

$$H(\hat{\sigma}) = 1 - \hat{\sigma}^\beta + (1 + \hat{\sigma}^{2\beta})^{\frac{1}{2}}, \tag{8.5}$$

and

$$\hat{\sigma}_{\hat{\xi}}(\hat{\xi}) = -(1 + (1 + \hat{\sigma}^{2\beta})^{\frac{1}{2}})^{-1}, \tag{8.6}$$

where $\hat{\sigma}$ takes values from the range $0 \leqslant \hat{\sigma} < \infty$. The boundary conditions are those to ensure matching where the monolayer/drop join as $\hat{\sigma} \to 0$, and matching with the solution given by (8.4) as $\hat{\sigma} \to \infty$. A simple case arises when $\beta = \frac{1}{2}$, then the solution of (8.6) may be written, implicitly, as

$$\hat{\sigma} + \tfrac{2}{3}(1 + \hat{\sigma})^{\frac{3}{2}} = \tfrac{2}{3} - \hat{\xi}, \tag{8.7}$$

which shows the required matching behaviour both as $\hat{\sigma} \to 0$ and as $\hat{\sigma} \to \infty$, e.g. as $\hat{\sigma} \to \infty$ then (8.7) implies that

$$\hat{\xi} \simeq -\hat{\sigma}^{\frac{3}{2}},$$

in accordance with the solution of (8.4) as $\sigma \to 0$ (when $\beta = \frac{1}{2}$). The general integral of (8.6) is cumbersome (it may be found in terms of incomplete β functions; see Abramowitz & Stegun 1972, p. 263) and is not pursued here.

To leading order in δ, ξ_ϵ is given by integrating (8.4), so

$$\xi_\epsilon = -\int_0^{1-\epsilon} \hat{\delta}^{-1}(\sigma)\, \mathrm{d}\sigma, \tag{8.8}$$

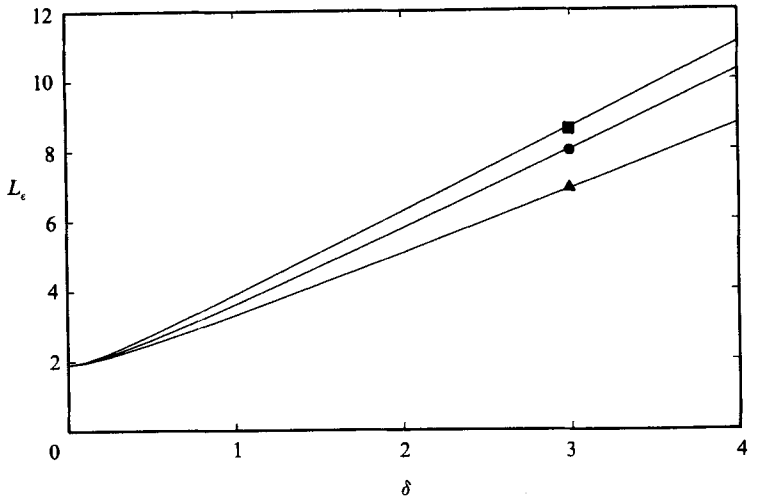

FIGURE 10. Effective monolayer length as a function of dimensionless dilute diffusivity constant, δ, for three different diffusion equations of state: as in figure 4 (●), as in figure 5 (▲) and for equation (6.3) ($n = 2$) (■).

where $\hat{\delta} = -\delta\tilde{\tilde{\delta}}$ which is independent of δ; corrections to ξ_ϵ will be of $O(\delta^{-\beta})$ but these are not calculated here. Moreover, the integral in (8.8) can be approximated to give

$$\xi_\epsilon = -\log\epsilon + O(1),$$

independently of the particular choice for the equation of state. Thus

$$L_\epsilon \simeq -\delta\log\epsilon \gg 2,$$

i.e. the effective monolayer length is very large, relative to the 'diffusionless' case. As mentioned, this example is of lesser importance than the former since surface-diffusion transport of contaminant is not expected to be the principle mechanism governing the monolayer dynamics.

9. Effective monolayer length

With L_ϵ defined by (7.7), and with ϵ chosen as 0.05, figure 10 shows curves for $L_\epsilon(\delta)$, as a function of δ, for three different equations of state for the diffusion coefficient. Curves 1 and 2 ($n = 4$ and 6 respectively) have diffusive mechanisms persisting for all surface concentrations of contaminant, while curve 3 shows the results for a system where surface diffusion is totally insignificant past the close-packing limit $\Gamma = 1$. For this latter case the exponent in the equation of state was chosen as $n = 2$; note that for $n \leqslant 1$ the solution gives an interface which has a discontinuous slope when $\Gamma = 1$.

The relative insensitivity of the results on the particular choice of equation of state indicates that the results obtained may exhibit fairly general trends for a wide class of possible equations of state. This robustness is essential given the crude nature of the model. The monolayer 'length', L_ϵ, is, however, a strong function of the dilute diffusivity D_0. The effective length is the primary practical result from the analysis, as shown in §10, estimates for spreading rates under fairly general conditions are influenced by the values of L_ϵ.

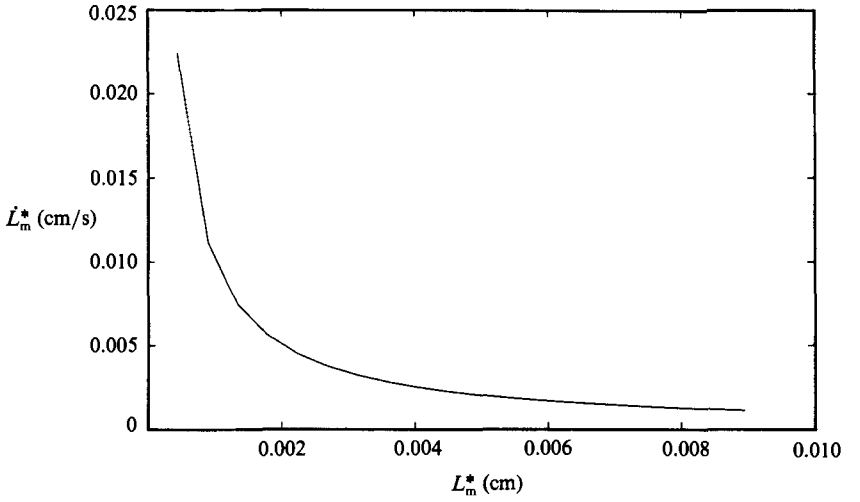

FIGURE 11. Spreading rate, $\dot{L}_m^*$, as a function of monolayer length, L_m^*, from equation (10.2); parameters: $S^* = 10$ dyn/cm, $h^* = 10^{-5}$ cm, $\mu_2^* = 10$ P and $\delta = 0.1$.

10. Spreading rates

From a practical point of view, determining how fast a monolayer spreads out is of much interest. While the problem considered above deals only with steady states, the solutions do, nevertheless, represent dynamical balances of the forces in question and therefore provide an order of magnitude estimate for the quasi-steady spreading case. The spreading rate is measured principally by the velocity of the 'tip' of the monolayer. Also, in two dimensions, the monolayer geometry is best characterized by the length of the monolayer, thus the spreading rate (rate of change of the monolayer length) needs to be characterized in terms of that length.

Let L_m^* be the effective length of the monolayer; therefore $\dot{L}_m^*$ is a measure of the spreading rate. We now imagine the monolayer spreading out with time, in a quasi-steady fashion; then we may identify L_m^* with U_w^* and, moreover, from §§5–9, the effective monolayer length may be written as

$$L_m^* = \frac{S^* h^*}{U_w^* \mu_2^*} L_e(\delta) \quad \left(\text{with } \delta = \frac{D_0^* \mu_2^*}{S^* h^*}\right), \tag{10.1}$$

so that the relationship

$$L_m^* \dot{L}_m^* = \frac{S^* h^*}{\mu_2^*} L_e(\delta) \tag{10.2}$$

holds. The right-hand side depends only on the material properties (i.e. S^*, D_0^*, μ_2^*) and the initial conditions (i.e. h^*); the purely numerical factor, $L_e(\delta)$, may be estimated from figure 10. Figure 11 shows a sample plot of the relationship given by (10.2), with parameter values as given above. Note that the spreading rate becomes increasingly small as the monolayer spreads out. This is because the gradients of surface tension become correspondingly small.

Integrating (10.2) provides an explicit relationship for the state of the monolayer with time:

$$L_m^*(t^*) = \left[2 \frac{S^* h^*}{\mu_2^*} L_e(\delta)\, t^*\right]^{\frac{1}{2}}. \tag{10.3}$$

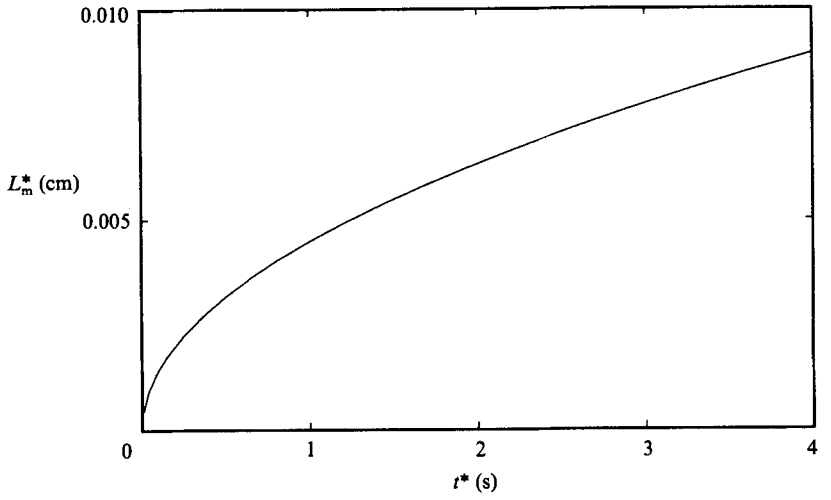

FIGURE 12. Monolayer length, L_m^*, as a function of time, t^*, from equation (10.3); parameters as in figure 11.

From (10.3) useful properties of the spreading process can be found, for example the total area covered as a function of time. A sample plot of relationship (10.3) is given in figure 12, with the parameter values as given above.

Note that such spreading implies an $O(t^{*\frac{1}{2}})$ growth in total contaminant mass in the monolayer, i.e. the bulk drop must continuously provide material for a monolayer that is spreading indefinitely. Therefore the quasi-steady assumption can only be valid provided that the bulk-droplet source is large enough to continually provide the necessary flux of material into the monolayer. This constraint may act to diminish spreading rates when, ultimately, the drop is depleted. Nevertheless, spreading as governed by equations (9.2) and (9.3) can be expected to be approximately valid for portions of the monolayer evolution.

Two-dimensional spreading with a $t^{*\frac{1}{2}}$ growth of the monolayer length has been observed experimentally. Ahmad & Hanson (1972), using oleic acid spreading on a glycerol layer (with $S^* = 20$ dyn cm^{-1}, $\mu_2^* = 10$ P and $h^* = 0.03$–0.12 cm (large)), found just such behaviour, and furthermore provided an *ad hoc* theory justifying the result. The $t^{*\frac{1}{2}}$ result is a very robust prediction, coming from dimensional analysis of (3.13) and (3.14). The theory of Ahmad & Hanson (1972) agrees with the experiments more closely, with result (10.3) overpredicting the spreading rate by a factor of $\sqrt{2}$. This is to be expected. The theory of Ahmad & Hanson (1972), however, suffers from unjustifiable assumptions, whereas the equations in §3 may be solved (ultimately) to provide fully unsteady solutions. Also we note that the regimes that Ahmad & Hanson (1972) investigate have parameter values that suggest that gravity should be important, in fact, α is $O(1)$ for the thicker layer; thus it is entirely fortuitous that the simple 'dimensional analysis' provides accurate results for the spreading rates.

11. Discussion

In the previous sections a steady-state problem was posed to address monolayer-spreading phenomena. Distributions of monolayer surface concentration, substrate height and surface velocity were obtained explicitly, as functions of the material

properties. In particular, dependence on surface diffusivity was highlighted with asymptotic results relevant for both small and large surface diffusivity obtained.

In the absence of surface diffusivity, the film thickness, film velocities and monolayer-concentration gradients are discontinuous at the leading edge of a finite length monolayer. When surface diffusion is present, the monolayer is infinitely long and now the dependent variables are everywhere continuous. The variation of surface tension occurs over a longer domain, hence the monolayer gradients of surface tension are smaller for $-2 < x < 0$ and larger for $x < -2$ when compared to the diffusionless case. In the interval $-2 < x < 0$, the reduction of these tractions, which oppose the shear force of the underlying moving film, leads to an increase in surface velocities. On the other hand, the region $x < -2$ experiences an increase in surface tractions leading to a decrease in surface velocities. Note that, in order to conserve mass, increases (decreases) of surface velocity require a corresponding decrease (increase) in film thickness. This explains the crossing of curves in the region $x < -2$ of figures 6–9.

Surface diffusion leads to successively faster spreading rates when systems of the same effective length, L_m^*, but successively larger diffusivities, are compared. The reason being that while the dynamic forces are essentially the same (same surface-tension variation over the same length) there is greater kinematic spreading due to the larger diffusive flux.

The main qualitative difference between the solutions obtained with the first set of equations of state examined and the second was the regularity of the solution near $x = 0$ (the monolayer-droplet boundary). It was noted earlier that steady-state solutions exist only if the diffusivity vanishes fast enough at large monolayer surface-concentrations. When this condition is just met ($n = 3^+$ in (6.2)) the solution changes rapidly near the bulk droplet boundary, but for sufficiently rapid fall (larger n) the solution will be smooth. Thus, in figures 6 and 8, for the case with $n = 4$, we see that slopes become large near $x = 0$, while for $n = 6$, as shown in figures 7 and 9, the slopes are always $O(1)$. Despite this qualitative difference the quantitative difference between the solutions for the respective equations of state is surprisingly small when far enough removed from $x = 0$. In fact only the details of the solution near $x = 0$ are sensitive to the form of the equation of state, furthermore, for quantities such as monolayer length which depend on integration of (7.4), the details about $x = 0$ are relatively unimportant and so from figure 10 curves for effective length are qualitatively similar. A general conclusion from figure 10, therefore, is that effective length increases approximately linearly with δ (at least for large enough δ) and consequently that the spreading rate increases like $\delta^{\frac{1}{2}}$ while decreasing with time like $t^{-\frac{1}{2}}$.

With regard to pulmonary mechanics the principle significance of this work is to provide parameters in order to assess similarity of bench top experiments and relevant lung lining flows. Those dimensionless parameters identified in §5 should be matched as closely as possible with the values appropriate for the lung (see §5) in order to mimic the mechanical properties of the lung.

This work was supported by the National Science Foundation Presidential Young Investigator Award MEA 8351491 in conjunction with General Motors Corporation, and the National Institutes of Health Research Career Development Award K04-HL-01818.

REFERENCES

ABRAMOWITZ, M. & STEGUN, I. A. 1972 *Handbook of Mathematical Functions*. Dover.

ADAMSON, A. W. 1967 *Physical Chemistry of Surfaces*, chapter 3. Wiley-Interscience.

ADLER, J. & SOWERBY, L. 1970 *J. Fluid Mech.* **42**, 549–559.

AHMAD, J. & HANSON, R. S. 1972 *J. Colloid Interface Sci.* **38**, 601–604.

BIENKOWSKI, R. & SKOLNICK, M. 1972 *J. Colloid Interface Sci.* **39**, 323–330.

COX, R. G. 1986 *J. Fluid Mech.* **168**, 195–220.

DI PIETRO, N. D., HUH, C. & COX, R. G. 1978 *J. Fluid Mech.* **84**, 529–560.

DI PIETRO, N. D. & COX, R. G. 1979 *Q. J. Mech. Appl. Math.* **22**, 355–381.

DI PIETRO, N. D. & COX, R. G. 1980 *J. Fluid Mech.* **96**, 613–640.

DUSSAN V, E. B. & DAVIS, S. H. 1974 *J. Fluid Mech.* **65**, 71–95.

FODA, M. & COX, R. G. 1980 *J. Fluid Mech.* **101**, 33–57.

GAINES, G. L. 1966 *Insoluble Monolayers at Liquid–Gas Interfaces*. Wiley-Interscience.

GREENSPAN, H. P. 1978 *J. Fluid Mech.* **84**, 125–143.

GROTBERG, J. B., MITZNER, W. A. & DAVIS, S. H. 1980 *J. Biomech.* **13**, 905–912.

HARKINS, W. D. 1952 *The Physical Chemistry of Surface Films*. Reinhold.

HUSSAIN, Z., FATIMA, M. & AHMAD, J. 1975 *J. Colloid Interface Sci.* **50**, 44–48.

LEVICH, V. G. 1962 *Physicochemical Hydrodynamics*. Prentice Hall.

SAKATA, E. K. & BERG, J. C. 1969 *I. & E. C. Fundamentals* **8**, 570–575.

SCHRECK, R. M. 1982 *Air Pollution: Physiological Effects*, pp. 183–219. Academic.

SCRIVEN, L. E. 1960 *Chem. Engng Sci.* **12**, 98–108.

SHELUDKO, A. 1966 *Colloid Chemistry*, chap. 6. Elsevier.

VON NEERGAARD, K. 1929 *Z. ges. Exper. Med.* **66**, 373.

WEST, J. B. 1979 *Respiratory Physiology – The Essentials*. Williams & Wilkins.

YIH, C.-S. 1969 *Phys. Fluids* **12**, 1982–1987.